Open Access

Journal of Energy and Power Technology

LIDSEN Publishing Inc.

Original Research

Development of Binderless Waste-Derived Briquettes: Effect of Plastic Content on Combustion Performance and Kinetics

Peter Ebhodaghe Akhator [1, 2, *], Ufuoma Georgina Unueroh [3]

1. Department of Mechanical Engineering, University of Benin, Benin City, Nigeria; E-Mail: peter.akhator@uniben.edu
2. Department of Chemical Engineering, University of Johannesburg, Johannesburg, South Africa
3. Department of Materials and Metallurgical Engineering, University of Benin, Benin City, Nigeria; E-Mail: georgina.odin@uniben.edu

* **Correspondence:** Peter Ebhodaghe Akhator; E-Mail: peter.akhator@uniben.edu

Academic Editor: Gasim Hayder

Special Issue: Bioenergy and Waste-to-Energy

Journal of Energy and Power Technology
2026, volume 8, issue 2
doi:10.21926/jept.2602009

Received: February 16, 2026
Accepted: May 07, 2026
Published: May 15, 2026

Abstract

Waste-derived briquettes offer a promising alternative to fossil fuels and are characterised by low production costs, high volumetric calorific value, robust mechanical strength, and excellent durability. To optimize their adoption, four variants of waste-derived briquettes were produced with different mass ratios of sawdust to polyethylene terephthalate (PET) plastic (100:0, 90:10, 80:20, and 70:30) using high-pressure compaction without binders. Thermogravimetric analysis (TGA) and the Coats-Redfern method were employed to investigate the impact of PET content on the combustion behavior and kinetics. In contrast, the water-boiling test was employed to identify their fuel efficiency and energy consumption. The ash content of the briquettes decreased with increasing PET content, reatching 2.62% in BR-D (30% PET plastic). The plastic-based briquettes contained significant amounts of alkali metal oxides, which were synergistically active in catalysing the combustion of the briquettes as indicated by decreases in the ignition temperature of 6-25°C and the burnout temperature of 88-165°C. The briquettes met the European Pellet Council (EPC) requirements of densified

solid fuels in terms of heavy-metal concentrations, except for the cadmium limit in BR-D, which was a little higher than the set limit. Moreover, the kinetic study indicated that briquettes containing PET exhibited lower activation energies (E_a) than those briquettes without PET. Notably, BR-D had the lowest E_a value of 18.67 kJ/mol. BR-D also had the highest energetic density (16.93 GJ/m^3) and fuel value index (6.46 GJ/m^3%), making it the most favourable for energy applications. This implies that blending waste PET plastics with sawdust could enhance the thermal efficiency and fuel quality of the resulting briquettes, making them potentially sustainable energy sources, both on their own and in combination with traditional fuels.

Keywords
Combustion; kinetics; PET plastics; sawdust; TGA; waste-derived briquettes

1. Introduction

Briquettes are becoming an important means of realizing the potential of biomass and various solid waste streams as a renewable energy source. A densification process produced them called briquetting, which involves compressing various biomass materials either singly [1, 2] or in combination [3-6] into a uniform and high-density structure. It is a physical method of converting irregular and crushed biomass into a smaller, more uniform form by applying mechanical and plastic deformation under well-controlled temperature, pressure, and moisture conditions. Briquettes have many advantages over raw biomass, such as higher density and calorific value, reduced emissions of greenhouse gases, including CO_2, N_2O, and SO_2, and a substantial reduction in toxic pollutants [2, 7]. They are denser and have lower volume, which enhances their handling, storage, and transportation efficiency [8, 9] and helps combat deforestation and ensure environmental sustainability [10].

Biomass briquettes are increasingly popular as an excellent substitute for traditional fuels such as firewood and charcoal for domestic heating, cooking, and industrial activities in urban and rural societies worldwide [11-13]. Plastic waste is an emerging, promising raw material for the production of briquettes, due to its high calorific value. For example, Cheremisinoff [14] reported that plastic waste has a calorific value of about 34 MJ/kg, higher than that of wood (about 20 MJ/kg) and paper waste (about 17 MJ/kg). Incorporating plastic waste into briquettes could increase their energy content and thermal performance, while alleviating environmental concerns related to plastic buildup, as plastic is non-biodegradable [5, 9, 15].

Several studies examined the incorporation of waste plastics into biomass or other solid wastes to enhance briquette characteristics [3, 5, 9, 16, 17]. Consistently, these studies indicated that the addition of plastic enhances the calorific value and mechanical strength of the briquettes and lowers the ash content. Despite these promising energy and mechanical performance indicators, plastic-biomass briquettes are yet to be widely adopted [18, 19]. This is probably due to inadequate knowledge of their combustion behaviour and kinetics. It is important to address these gaps to optimize briquette design, improve operational efficiency, and promote consumer acceptance of waste-plastic-based briquettes.

Thermogravimetric analysis (TGA) is a common technique for studying the thermal degradation and energy release properties of solid fuels, including briquettes. Studies that have used thermogravimetric methods have typically indicated positive combustion behaviour and clear kinetic characteristics, highlighting the possibility of briquettes as a sustainable fuel source [2, 7, 20, 21]. Indicatively, Jia [20] examined briquettes obtained from different types of biomass, including masson pine, Chinese fir, willow, slash pine, and poplar, and recorded activation energies between 56 and 542 kJ/mol by the Coats-Redfern method. Equally, Yiga et al. [2] examined carbonized rice husk briquettes prepared by low-pressure methods and cassava flour binder and found that the activation energies were 75-83 kJ/mol. Qi et al. [7] demonstrated that briquetting enhanced combustion efficiency and decreased pollutant emissions such as SO_2 and NO, with high goodness-of-fit measures (>0.99) using the Coats-Redfern kinetic analysis. Bongomin et al. [22] performed elaborate analyses of the thermal decomposition of five biomass wastes, coffee husk, groundnut shell, macadamia nutshell, rice husk, and tea waste, using TGA coupled with the Coats-Redfern method. Their findings showed that macadamia shells were the most reactive to thermal degradation, and coffee husk was the most difficult to degrade, with thermodynamic parameters indicating a high enthalpy change but a low Gibbs free energy.

Moreover, Liu et al. [21] examined the combustion and kinetic behaviour of briquettes prepared from corn straw at various heating rates. They reported excellent combustion performance, with activation energies of approximately 109-114 kJ/mol, based on Flynn-Wall-Ozawa (FWO), Friedman, Starink, and Kissinger-Akahira-Sunose (KAS) methods. Nevertheless, research directly focused on briquettes made from mixtures of plastics and sawdust is limited, and systematic research on the impact of different plastic concentrations on their combustion characteristics and kinetics is lacking. Filling this knowledge gap is crucial for optimising such briquette formulations, enhancing combustion performance, and advancing their eco-friendly utilization.

In this study, binderless briquettes were made using high-pressure compaction (~17 MPa) of mixtures of sawdust and waste PET plastics, and their combustion performance and kinetics were evaluated. Additionally, characterisations based on physicochemical analysis, SEM, FTIR, durability, and energetic parameters were provided. The insights from this study are intended to inform the development and optimization of briquette production and their combustion systems, to achieve cleaner, more efficient energy solutions in the future.

2. Materials and Methods

2.1 Raw Materials Collection and Preparation

Sawdust (emanating from the processing of different tree species) and discarded polyethylene terephthalate (PET) plastic bottles are the primary materials utilized in this study for briquette production. The PET bottles were collected from waste receptacles in Benin City, Edo State, Nigeria. The tops and labels of the bottles were removed to ensure uniformity before heating them at 230°C to facilitate melting. The molten PET was held at that temperature for 5 minutes before being allowed to cool for 10 minutes, and thereafter pulverized into powder using a locally fabricated pulverizer. The powder was sieved using a lab sieve with a 50 µm mesh to obtain a uniform grain size (see Figure 1a). The sawdust was obtained from the sawmill's dumpsite in Benin City, Nigeria. It was sieved using a lab sieve with a 50 µm mesh to obtain a uniform particle size (see Figure 1b).

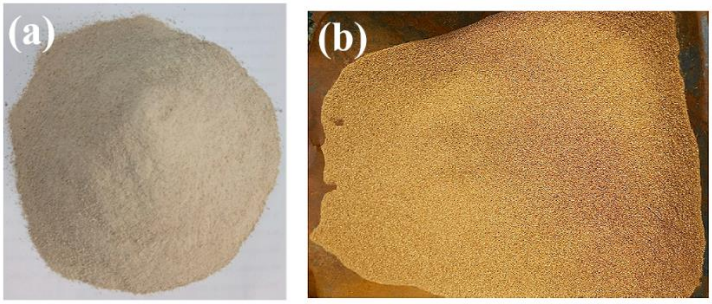

Figure 1 Prepared biomass samples used in this study (a) sieved PET powder, (b) sieved sawdust.

2.2 Briquettes Production

The PET powder (PP) and sieved sawdust (SD) were mixed at four *mass* ratios as illustrated in Table 1 to yield four types of briquettes: BR-A, BR-B, BR-C, and BR-D. No binder was used in this study.

Table 1 The briquette types and their mixing ratios.

Briquette Type	Mixing ratios (wt.%)
BR-A	100% SD and 0% PP
BR-B	90% SD and 10% PP
BR-C	80% SD and 20% PP
BR-D	70% SD and 30% PP

One hundred grams of each blend was carefully placed in a plastic bucket and thoroughly stirred by hand with a wooden spatula until a uniform, consistent blend was achieved. The homogeneous mixture was transferred into a high-pressure hydraulic press briquetting machine (~17 MPa), where it was compressed to form compact, densified briquettes, as shown in Figure 2. The briquetting machine produces 50 briquettes per hour. The briquettes, which are 4.5 cm in diameter, have heights ranging from 1.5 cm to 3.7 cm.

Figure 2 Produced PET-wood waste briquettes.

2.3 Analysis of Physicochemical Properties, Ash Composition, and Heavy Metals Concentration

The carbon (C), hydrogen (H), nitrogen (N), and sulphur (S) contents of both the raw materials and briquettes were determined using an elemental analyser (Exeter, EA-1110) following ASTM D5373-02 standards, while the oxygen content was calculated using Equation (1).

$$O\% = 100 - (N + C + H + S + ASH)\% \quad (1)$$

The proximate properties of the biomass samples were determined using a thermogravimetric analyzer (NETZSCH-STA449F5) with a sample amount of 12 ± 0.5 mg. following the ASTM E1131-08 standard. The analyser was run until constant weights were recorded. This residual weight is the ash content. Percentage ash content was calculated using Equation (2).

$$\%Ash = \frac{mass\ of\ residual\ ash}{initial\ mass\ of\ sample} \quad (2)$$

An oxygen bomb calorimeter (CAL3K-A) was used to measure the samples' higher heating values (HHV). Each experiment was repeated three times.

The ash composition of the briquettes was analyzed using an energy-dispersive X-ray fluorescence (XRF) spectroscopy (Rigaku RIX-3000, Japan). The concentrations of heavy metals in the briquettes were determined using an atomic absorption spectrometer (GBC, Avanta-PM) and compared with European standards. Table 2 shows the ash composition of the briquettes.

Table 2 Ash composition of produced briquettes.

Ash analysis	**Briquettes**			
(wt.%, dry basis)	**BR-A**	**BR-B**	**BR-C**	**BR-D**
MgO	0.5710	0.9993	0.7744	0.7416
Al_2O_3	2.6533	3.5162	4.0847	3.3929
SiO_2	6.8531	8.8915	12.7458	16.0140
P_2O_5	1.4977	1.8400	1.4228	1.8219
SO_3	0.2980	0.4125	0.4080	0.2665
Cl	0.4306	1.1918	1.3323	1.9829
K_2O	4.9666	14.2265	8.9761	12.6989
CaO	9.0059	28.7605	20.6127	26.5501
TiO_2	40.2535	2.7656	2.6308	2.9141
Cr_2O_3	4.1114	2.4624	1.5993	3.4230
MnO	1.3870	0.9974	0.8468	-
Fe_2O_3	20.6610	29.3862	41.4635	24.4965
ZnO	1.1268	0.8380	1.2370	1.4213
Rb_2O	-	0.3382	-	-
SrO	-	-	0.7671	-
ZrO_2	-	-	-	0.8076

2.4 Mechanical Characterization of the Briquettes

To evaluate the structural integrity of the briquettes, they were lifted to a height of 2 meters and then dropped onto a sturdy concrete floor to simulate a standardized, controlled method to assess their mechanical strength and durability under impact conditions similar to those encountered in real-world handling stresses, such as transportation, handling, and storage. The mechanical strength was calculated by dividing the briquette's weight after dropping by its weight before dropping. Additionally, the briquettes' particle density was determined using standard methods based on the mass-to-volume ratio. Each characterization experiment was performed three times.

2.5 Morphology Studies and FTIR Spectrometry

The morphologies of the briquettes were analyzed using Scanning electron microscopy (SEM) microphotographs, obtained with a Thermo Scientific Phenom ProX scanning electron microscope, PhenomWorld, Eindhoven, Netherlands. The briquette samples were placed on the aluminum holder stub using sticky carbon tape, then vacuum-dried and scanned at an acceleration voltage of 15 kV. The surface functional groups of the samples were analyzed by Fourier transform infrared (FTIR) spectroscopy on a ThermoFisher Scientific iS50 FTIR spectrometer, which scans from 4000 to 400 cm^{-1} at a resolution of 4 cm^{-1} and a scanning speed of 2 mm/sec. The briquettes were ground into fine powders before the FTIR analysis.

2.6 Analysis of Combustion Properties of the Briquettes

The combustion properties of the produced briquettes were examined using a thermogravimetric analyzer (NETZSCH-STA449F5). The analyzer operates from room temperature to 1600°C and can operate with nitrogen, oxygen, or air. The briquettes were ground and sieved through a laboratory test sieve to particle sizes ranging from 50 to 70 µm. About 10 ± 0.5 mg of each briquette type was weighed, placed into a platinum crucible and inserted into the thermogravimetric analyser. The samples were heated from ambient temperature to 900°C at 10°C/min in an oxygen atmosphere at 100 mL/min. The resulting data were used to generate TG and DTG curves for all samples.

Several key combustion parameters, including the ignition temperature (T_i), peak temperature (T_p), and burnout temperature (T_b), were extracted from the TG and DTG curves to evaluate the overall combustion performance of the briquettes. T_i is typically determined using the tangent method on the TG-DTG curves [23]. Furthermore, three combustion indices, namely, the ignition index (D_i), burnout index (D_b), and combustion intensity index (H_f), were evaluated during the combustion analysis. These indices were calculated using Equations (3)-(5) [23, 24].

$$D_i = \frac{DTG_{max}}{t_i t_p} \tag{3}$$

$$D_b = \frac{DTG_{max}}{t_b t_p \Delta t_{1/2}} \tag{4}$$

$$H_f = T_p \times 10^{-3} \ln\left(\frac{\Delta T_{1/2}}{DTG_{max}}\right) \tag{5}$$

where DTG_{max} = highest weight loss rate (wt.%/°C), t_i = time taken to ignite (min), t_b = time taken to burnout (min), $\Delta T_{1/2}$ = temperature range at half of DTG_{max} value (°C), $\Delta t_{1/2}$ = time range at half of DTG_{max} value (min), t_p = time to reach peak temperature (min).

2.7 Combustion Kinetic Modeling

Kinetic analysis is very important in the study of the combustion process of solid fuels, including briquettes. In this study, the Coats-Redfern method was used to estimate kinetic parameters from TGA data. It was selected for its strength, ease, and efficiency in non-isothermal conditions characteristic of biomass thermal degradation [25]. It is especially appropriate for analyzing data obtained at a single heating rate, which aligns with our experimental design. The reaction rate constant (k) is dependent on absolute temperature (T), which is expressed by the Arrhenius equation [26]:

$$k(T) = A\exp\left(-\frac{E_a}{RT}\right) \tag{6}$$

T indicates the temperature (K), *A* signifies the pre-exponential factor (min^{-1}), E_a indicates the activation energy (kJ/mol), and *R* is the universal gas constant (0.008314 kJ/mol K). The solid-gas reaction rate is defined as follows [26]:

$$\frac{dx}{dt} = k(T) \cdot g(x) \tag{7}$$

$\frac{dx}{dt}$ represents the rate of degradation, which is a linear function of the temperature rate constant. *x* represents the briquettes' weight loss ratio during the combustion, *t* signifies the time for the combustion, and *g(x)* is the differential form of the reaction model, which depends on the reaction mechanism. The weight loss ratio *(x)* can be obtained from thermogravimetric analysis data, as follows [27]:

$$x = \frac{m_0 - m_t}{m_0 - m_f} \tag{8}$$

m_0, m_t, and m_f are the initial, instantaneous, and residual mass of samples during the combustion process, respectively.

Combining Equations (6) and (7) at the heating rate ($\beta = dT/dt$) and rearranging gives Equation (9):

$$\frac{dx}{dT} = \frac{A}{\beta}\exp\left(-\frac{E_a}{RT}\right) g(x) \tag{9}$$

The integral expression of *g(x)* is presented in Equation (10).

$$f(x) = \int_0^x \frac{dx}{g(x)} = \frac{A}{\beta}\int_{T_0}^{T} \exp\left(-\frac{E_a}{RT}\right) dT \tag{10}$$

A = pre-exponential factor (min^{-1}), E_a = activation energy (kJ/mol), $k(T)$ = reaction rate constant, R = universal gas constant, T = reaction temperature (K), x = conversion rate, and $g(x)$ = kinetic model, $f(x)$ = the integral form of the kinetic model.

Kinetic parameters, such as the activation energy, can be determined by integrating Equation (10) and approximating the exponential term. For the Coats-Redfern method, after approximation and rearrangement, the solution is expressed as Equation (11) [27]:

$$\ln\frac{f(x)}{T^2} = \ln\frac{AR}{\beta E_a} - \frac{E_a}{RT} \tag{11}$$

In this study, the briquettes' combustion process was approximated as a first-order kinetic reaction; hence, according to [27],

$$g(x) = 1 - x \tag{12}$$

Substituting in Equation (10) and integrating, Equation (11) translates to:

$$\ln\left[-\frac{\ln(1-x)}{T^2}\right] = \ln\frac{AR}{\beta E_a} - \frac{E_a}{RT} \tag{13}$$

Straight lines were fitted from the plots of $\ln\left[-\frac{\ln(1-x)}{T^2}\right]$ against $\frac{1}{T}$, and the activation energy (E_a) was estimated from the slope $\left(-\frac{E_a}{R}\right)$ of the plots.

2.8 Water Boiling Test (WBT)

Version 4.2.3 of the Water Boiling Test (WBT) protocol was used to ascertain the thermal performance of the developed briquettes practically. An upgraded cookstove was used, and the performance evaluation involved boiling 5 litres of water in a flat-bottomed, cylindrical aluminium cooking pot with a maximum capacity of 7 litres. The tests were carried out using the briquette samples, like typical household cooking methods. Specific operational parameters, such as thermal efficiency, time to boil, specific fuel consumption, burning rate, and firepower, were evaluated for all three WBT phases: cold-start high-power phase, hot-start high-power phase, and simmer low-power phase [28]. During high-power (cold start) conditions, 5 litres of water were heated to its boiling point in the 7-litre pot using the cookstove at room temperature. For the high-power (hot start) phase, 5 litres of water were heated to boiling point temperature in a 7-litre pot with the cookstove pre-heated, and during the simmer phase, the water temperature was kept at about 3°C below boiling point for 45 minutes [28]. Kerosene was used for igniting the briquettes during the test.

2.9 Energetic Characterization

The energetic densities (energy per unit volume) of the developed briquettes were determined by multiplying their particle density (PD) with their higher heating value (HHV), as shown in Equation (14) [2].

$$ED = PD \times HHV \tag{14}$$

where *ED* is the energetic density (MJ/m^3), *PD* is the particle density (kg/m^3), and *HHV* is the higher heating value (MJ/kg).

The Fuel Value Index (FVI) of the developed briquettes was determined using Equation (15) [2].

$$FVI = \frac{ED}{Ash} \tag{15}$$

where *FVI* is fuel value index (MJ/m^3%), and *Ash* is the Ash content of the briquettes (%).

3. Results and Discussion

3.1 Physicochemical Properties of Raw Materials and Briquettes

Table 3 presents the physicochemical properties of both the raw materials and the briquettes (BR-A to BR-D) produced in this study. PET plastic is known to contain a high proportion of volatile matter (VM) due to its manufacturing process and chemical composition [29, 30]. Consequently, the VM content of PET waste was substantially higher than that of sawdust, thereby directly impacting the overall VM levels in the briquettes. Specifically, the VM percentage increased with increasing plastic content, rising from approximately 83.19% in BR-B to 85.19% in BR-D, as indicated in Table 3. These observations are consistent with findings from previous studies [3, 17].

Table 3 Physicochemical properties of the produced briquettes.

	Raw materials		Briquettes			
	PET	**SD**	**BR-A**	**BR-B**	**BR-C**	**BR-D**
Proximate analysis						
VM	87.8 ± 0.15	78.33 ± 0.12	81.54 ± 0.13	83.19 ± 0.12	85.08 ± 0.15	85.19 ± 0.13
FC	5.02 ± 0.20	8.26 ± 0.19	8.63 ± 0.21	6.84 ± 0.15	7.85 ± 0.17	8.04 ± 0.20
MC	5.09 ± 0.12	7.78 ± 0.15	4.35 ± 0.15	6.84 ± 0.17	4.12 ± 0.12	4.14 ± 0.15
Ash	2.09 ± 0.03	5.63 ± 0.02	5.48 ± 0.05	3.13 ± 0.03	2.95 ± 0.02	2.62 ± 0.05
Ultimate analysis						
C	60.55 ± 0.12	47.58 ± 0.15	48.55 ± 0.15	55.58 ± 0.12	56.85 ± 0.17	57.87 ± 0.15
H	3.02 ± 0.11	6.32 ± 0.15	5.73 ± 0.12	5.55 ± 0.10	5.12 ± 0.15	4.95 ± 0.12
N	0.08 ± 0.15	0.06 ± 0.12	0.06 ± 0.12	0.06 ± 0.12	0.06 ± 0.10	0.06 ± 0.10
S	-	-	-	-	-	-
O	*34.26 ± 0.21*	*40.41 ± 0.20*	*40.18 ± 0.22*	*35.68 ± 0.18*	*35.02 ± 0.22*	*34.26 ± 0.22*
Atomic ratios						
H/C	0.050 ± 0.03	0.133 ± 0.02	0.118 ± 0.02	0.099 ± 0.05	0.090 ± 0.05	0.086 ± 0.02
O/C	*0.566 ± 0.05*	*0.849 ± 0.04*	*0.828 ± 0.05*	*0.642 ± 0.04*	*0.616 ± 0.04*	*0.596 ± 0.03*
HHV (MJ/kg)	25.05 ± 0.21	19.85 ± 0.21	20.00 ± 0.25	21.55 ± 0.18	22.12 ± 0.22	23.65 ± 0.20

FC was observed to be the highest in BR-A, probably due to the high amount of FC in SD. It was, However, it was observed to increase from 6.84% in BR-B to 8.05% in BR-D as the PET content increased. All samples had lower FC than BR-A, probably because the raw sawdust contained higher FC. Table 3 also summarises the elemental composition analysis. The carbon content and heating value of PET waste were higher than those of the sawdust, which was probably attributable to the chemical composition and structure of plastics [14]. This had a significant impact on the carbon content and HHV of the plastic-containing briquettes, as indicated in Table 3. The ratio of plastic in

the briquette blends was positively correlated with the carbon content and heating value in the samples BR-B to BR-D, with carbon content increasing from 48.55 to 57.87% and heating value rising from 20 to 23.65 MJ/kg. These findings are consistent with previous studies [5, 17, 31]. The hydrogen and oxygen content of the briquettes was comparable among samples, as indicated in Table 3. No significant amounts of nitrogen were detected, and no sulphur was detected at all, which means that these briquettes are not expected to generate significant amounts of nitrogen oxides (NO_x) during the combustion or co-combustion process [5, 32].

3.2 Fuel Characteristics of the Produced Briquettes

As indicated in Table 3, the atomic ratios of the hydrogen to carbon (H/C) and oxygen to carbon (O/C) in the briquettes were between 0.086 and 0.118 and 0.828 to 0.596, respectively. These ratios were plotted on the Van Krevelen diagram (Figure 3), which graphically illustrated the evolution of the composition and fuel properties of the briquettes [33]. Reduced ratios usually indicate improved fuel quality, as reflected by the proximity to the origin of the diagram [33, 34]. The briquette produced from sawdust alone (BR-A) was initially located in the upper right-hand corner, as is typical of biomass. Upon mixing with PET plastics, the samples moved toward the origin, indicating greater levels of coalification, higher energy density, and better solid-fuel prospects [35]. The diagram also indicates that the rise in plastic content shifts briquettes from the lignite area (BR-B) to the bituminous coal area (BR-C and BR-D). Comprehensively, the addition of PET plastic increases the coalification and consequently the quality of the fuel of the briquettes.

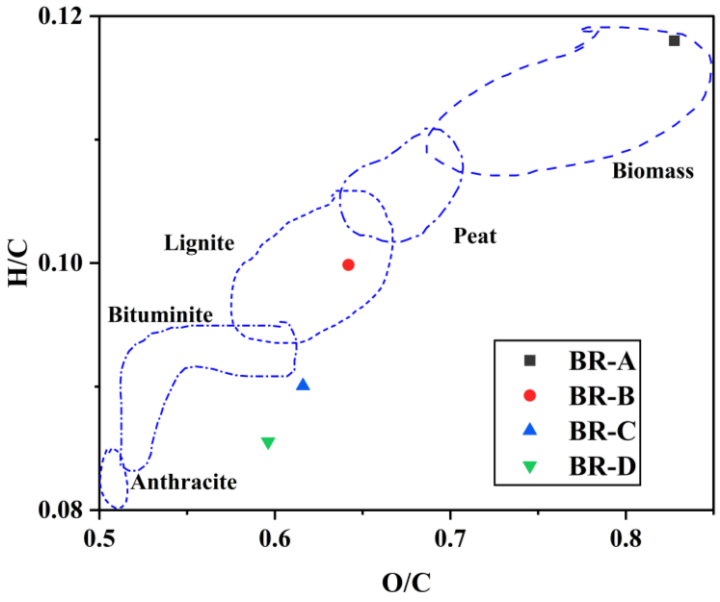

Figure 3 Van Krevelen diagram of produced briquettes.

From Table 3, the O/C ratios of the briquettes decreased from 0.828 in BR-A to 0.596 in BR-D, indicating significant de-oxygenation, which leads to an increase in higher energy density [4, 36]. Hence, BR-D shows the highest HHV. The lower O/C ratio in BR-D (0.596) indicates it is the most hydrophobic of the briquettes [37, 38]. It will be the least likely to absorb moisture from the air, making it the most stable for long-term storage in humid environments without crumbling or losing quality. The H/C ratios dropped from 0.11 to 0.08 from BR-A to BR-D, as seen in Table 3. These

remarkably low ratios suggest that the briquettes will burn with very little flame and minimal smoke. They will provide a steady, glowing heat rather than a rapid, volatile-driven fire [38, 39].

3.3 Mechanical Characterisation of the Briquettes

Table 4 presents the drop strengths and densities of the briquettes produced in this study. The data reveal that the drop strength and density of the briquettes increase with increasing plastic content. Specifically, the drop strength increases from 77.8% in BR-A (sawdust only) to 82.9% in BR-D (highest plastic content), implying improved mechanical durability and resistance to breakage during handling and transportation. The bulk density also shows a significant upward trend, increasing from 648.12 kg/m^3 in BR-A to 715.83 kg/m^3 in BR-D, which indicates enhanced compactness and energy density of the briquettes. Yiga et al. [2] observed a rise in density and mechanical strength for briquettes produced from carbonised rice husk.

Table 4 Drop strength and density of produced briquettes.

Briquette	Drop strength (%)	Density (kg/m^3)
BR-A	77.8 ± 0.26	648.12 ± 0.12
BR-B	78.5 ± 0.21	672.15 ± 0.13
BR-C	80.2 ± 0.12	709.21 ± 0.13
BR-D	82.9 ± 0.20	715.83 ± 0.12

3.4 Heavy Metal Concentration

Table 5 presents the concentrations of heavy metals in the produced briquettes. The results confirm that the concentrations of heavy metals in the briquettes comply with the standards set by the European Pellet Council (EPC) [40] for densified solid fuels. However, the cadmium content in BR-D was slightly above the set limit.

Table 5 Heavy metal concentrations of the produced briquettes.

Samples	Concentrations of heavy metals in the briquettes (mg/kg)			
	Cd	**Cr**	**Cu**	**Zn**
Limits*	≤0.5	≤10	≤10	≤100
BR-A	0.214	0.034	0.314	1.29
BR-B	0.385	0.036	0.488	2.45
BR-C	0.314	0.045	0.284	5.7
BR-D	0.574	0.075	0.875	7.8

*The limits set by the European Pellet Council for densified solid fuels.

3.5 FTIR Spectroscopy Results

Figure 4 shows the FTIR spectra of the developed briquettes.

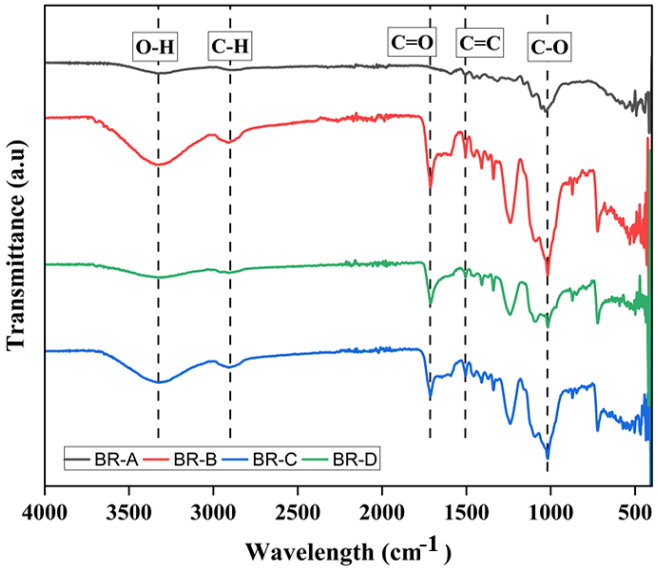

Figure 4 FTIR spectra of developed briquettes.

The FTIR spectra of the briquettes provide a detailed view of their chemical composition by showing characteristic absorbance bands associated with specific functional groups and molecular structures. For all samples, there's a broad band near 3400 cm^{-1}, which comes from O-H stretching vibrations, mainly due to moisture or hydroxyl groups present in the biomass. Interestingly, as the PET content increases, this band decreases in intensity, possibly indicating fewer hydroxyl groups in PET than in the biomass. In the 2900-2800 cm^{-1} range, signals related to aliphatic C-H stretching vibrations are observed, which are common in components like cellulose, hemicellulose, lignin, and the hydrocarbon chains in PET. These signals remain fairly consistent across all spectra, with minor variations that suggest changes in aliphatic content as PET content increases. A key feature appears around 1700 cm^{-1} in the spectra of briquettes with higher PET levels (BR-B, BR-C, BR-D). This peak corresponds to ester carbonyl groups (C=O), which are a hallmark of PET. Its increasing intensity with higher PET ratios confirms the presence of ester functionalities typical of PET plastics.

Furthermore, in spectra with more PET, especially those with higher ratios, there are noticeable peaks in the 1600-1500 cm^{-1} range. These are associated with aromatic C=C stretching vibrations, reflecting the aromatic rings within PET molecules. This peak is less prominent in the pure sawdust sample (BR-A), which mainly contains lignin and other biomass components. Finally, the bands between 1200 and 1000 cm^{-1} are linked to C-O stretching vibrations in esters, ethers, and carbohydrates. PET's ester groups add or strengthen these peaks, highlighting its chemical influence on the briquettes. According to Carnaje et al. [41], the detection of both aliphatic and aromatic hydrocarbons suggests the briquettes contain fats and oils, which can help improve their ignition properties.

3.6 Surface Morphologies of the Briquettes

Figure 5 presents SEM micrographs showing the morphology and structure of the produced briquettes. The SEM micrographs reveal notable morphological differences between the briquettes, which are probably attributable to the increasing content of PET plastics, acting as an effective binder and densifying agent.

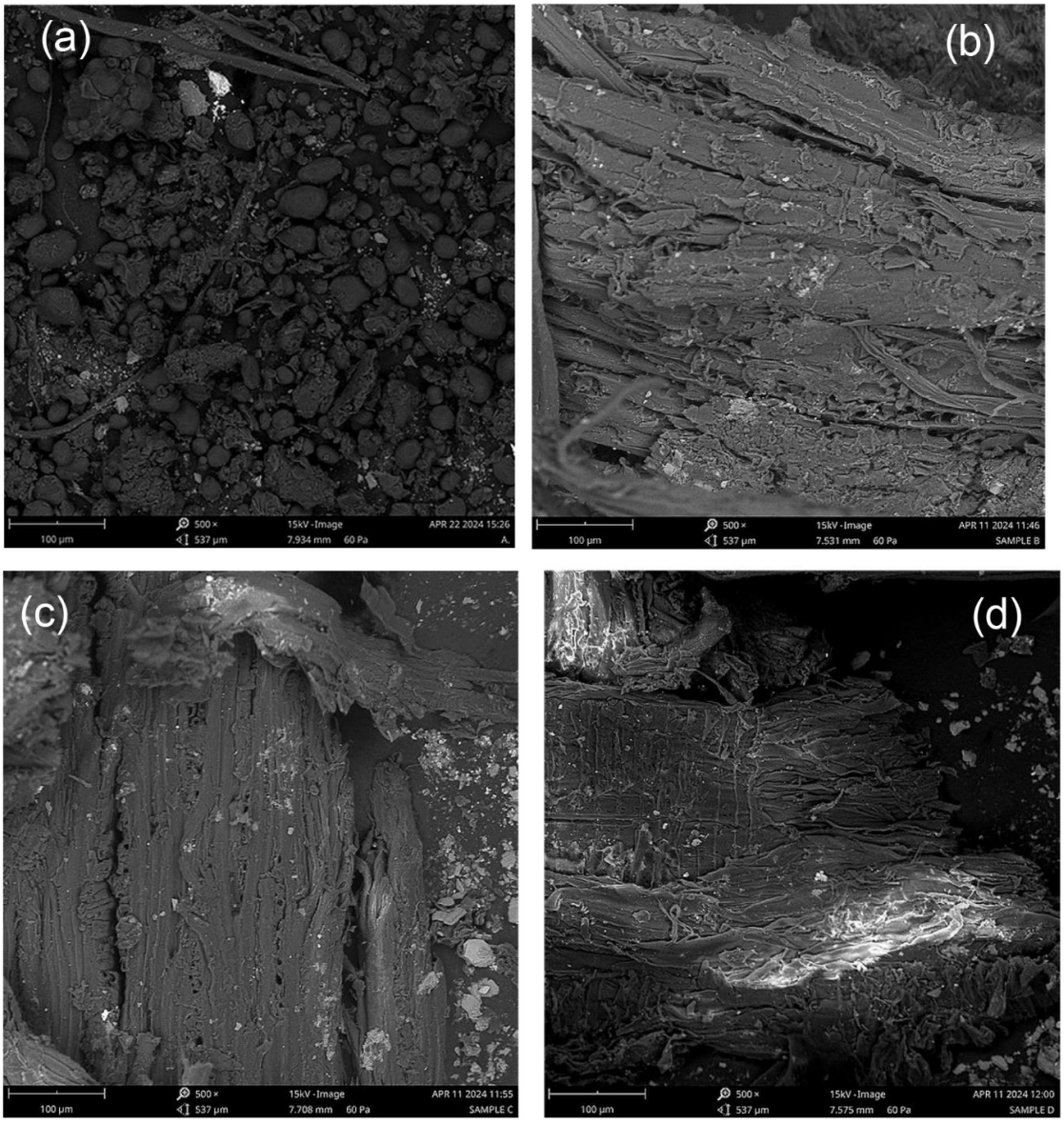

Figure 5 SEM micrographs of produced briquettes (a) BR-A, (b) BR-B, (c) BR-C, and (d) BR-D.

The micrograph (a) shows that the briquette made entirely of sawdust (BR-A) has a very porous and loose structure. The sawdust particles are clearly visible, irregular in shape, and many large gaps seperate them. This suggests that, without any binding agent, the particles don't stick together very well.

From micrographs (b) to (d), it can be observed that the structure of briquettes with more PET, progressing from BR-B to BR-D, becomes noticeably denser, more tightly packed, and more uniform. The images reveal that the sawdust fibres are being compressed and wrapped in a smoother material, probably the melted and re-solidified PET plastic. This layer fills the gaps and helps bond the particles much more strongly. Overall, increasing the PET content from BR-A to BR-D results in a clear transition from a porous, loosely held-together structure to a denser, layered, and more cohesive one. This enhanced density and bonding make the briquettes more durable and less prone to breaking apart or disintegrating. The layered, fibrous composition also promotes more controlled and stable burning, which could reduce emissions and improve fuel efficiency.

In particular, briquettes with higher PET, like BR-C and BR-D, are likely to be stronger during handling and storage, and to burn more evenly and efficiently. This means they might burn longer and produce cleaner, more consistent emissions. The SEM images clearly show that adding PET improves internal cohesion and reduces porosity, thereby enhancing physical and thermal performance. On the other hand, pure biomass briquettes are more porous and fragile, which negatively affects their durability. Overall, as the PET content increases, the structure improves, making these PET-sawdust composites a promising option for sustainable, high-performance fuels.

3.7 Thermogravimetric Analysis

Figure 6 presents the non-isothermal combustion behaviour of the briquettes (BR-A to BR-D) recorded using a thermogravimetric analyser (TGA). Table 6 presents key combustion parameters, including the ignition temperature (T_i), peak temperature (T_p), and burnout temperature (T_b). As shown in Figure 6, the briquettes initially experienced weight loss predominantly due to the evaporation of moisture and some volatiles, consistent with previous studies [7, 21]. This initial weight loss occurred over approximately 26 to 344°C for BR-A, 28 to 324°C for BR-B, 26 to 330°C for BR-C, and 26 to 319°C for BR-D. The initial weight reduction was approximately 9.79% for BR-A, 10.25% for BR-B, 9.07% for BR-C, and 6.69% for BR-D.

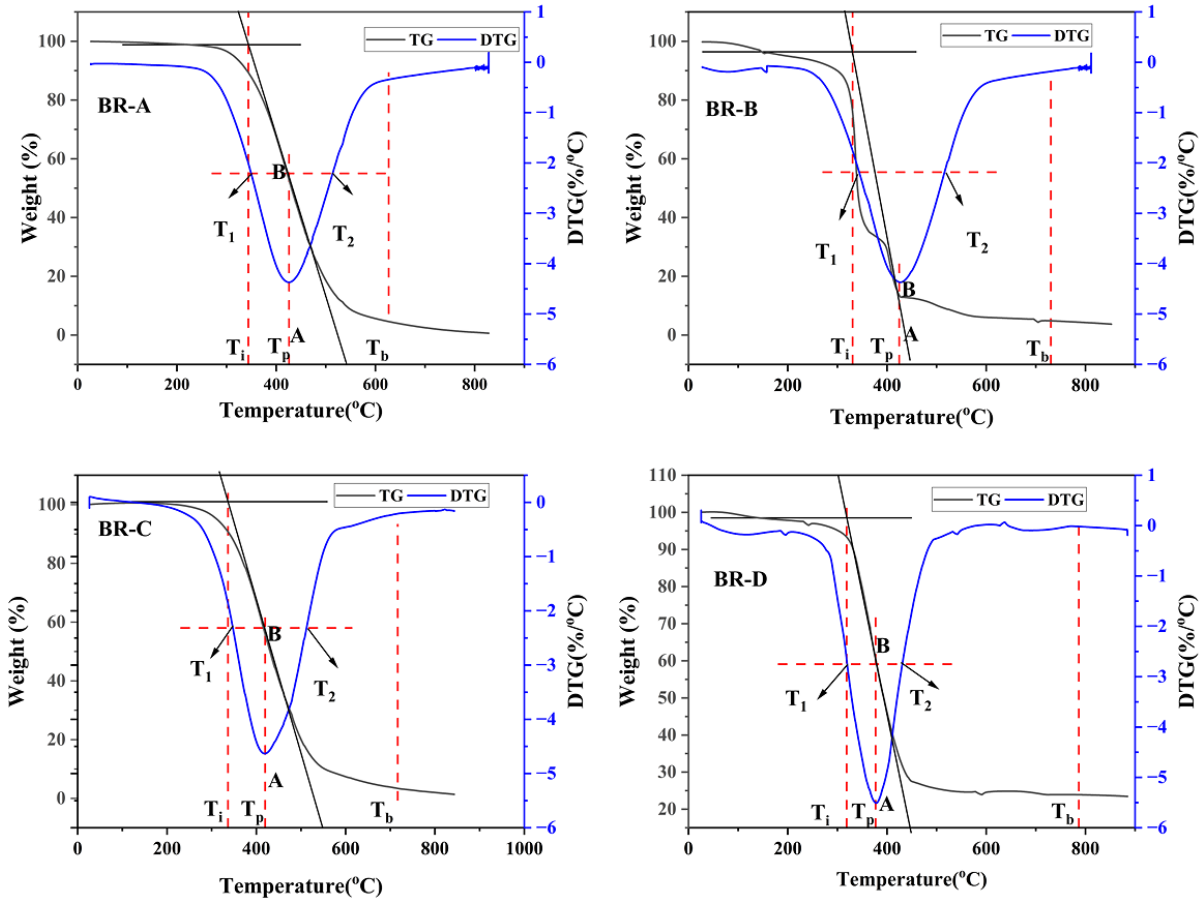

Figure 6 TG-DTG curves of the produced briquettes (BR-A to BR-D). T_i: ignition temperature (°C), T_p: peak temperature (°C), T_b: burnout temperature (°C), T_1: initial temperature at the medium point of maximum combustion rate, T_2: final temperature at the medium point of maximum combustion rate.

The evaporation of moisture led to the formation of cracks on the briquettes' surfaces, which subsequently facilitated the release of volatile compounds [42].

Table 6 Combustion parameters for the various briquette types.

Parameters	BR-A	BR-B	BR-C	BR-D
Ignition temperature (T_i, °C)	344	324	330	319
Peak temperature (T_p, °C)	426	424	420	377
Burnout temperature (T_b, °C)	625	713	732	790
Ignition time, (t_i, min)	9.00	8.00	8.50	7.50
Peak time (t_p, min)	17.25	17.15	17.00	15.75
Burnout time (t_b, min)	30.25	34.75	35.75	38.75
DTG_{max} (%/°C)	4.37	4.37	4.63	5.49
DTG_{mean} (%/°C)	1.08	1.07	1.07	0.83
Initial temperature at the medium point of maximum combustion rate (T_1, °C)	350	345	347	320
Final temperature at the medium point of maximum combustion rate (T_2, °C)	514	516	513	431
Medium point temperature range ($\Delta T_{1/2}$, °C)	164	171	166	111
Time at final temperature, T_2 (t_2, min)	17.00	17.50	16.98	15.00
Time at initial temperature, T_1 (t_1, min)	13.80	13.50	13.50	12.75
Medium point time range ($\Delta t_{1/2}$, min)	3.20	3.50	3.48	2.25

3.7.1 Effects of Plastic Concentration on T_i, T_p and T_b

The ignition temperature (T_i) for briquettes BR-A through BR-D is shown in Figure 7a. The data reveal that as the PET content increases, the ignition temperature tends to decrease. In particular, BR-D has the lowest ignition temperature at 319°C. The ΔT values show how much lower the ignition temperature is than that of BR-A, which contains no PET. For BR-D, this reduction is quite significant, about 25°C lower. This suggests that adding PET makes the briquettes easier to ignite. That's likely because PET is combustible and requires less energy to start burning. In solid fuels, higher amounts of volatile matter, fixed carbon, and oxygen generally facilitate ignition. During the initial stages of combustion, volatile substances are released from the fuel's surface, which then help promote burning. The fixed carbon, which burns more steadily, can keep the fire going once it's started, especially when fueled by those earlier-released volatiles. According to Table 3, BR-D has the highest volatile matter content at 85.19%. When these volatiles are released, they increase the briquette's porosity, creating a larger reactive surface area. This makes it easier for oxygen to interact with the fuel, speeding combustion, reducing resistance, and lowering the overall ignition temperature.

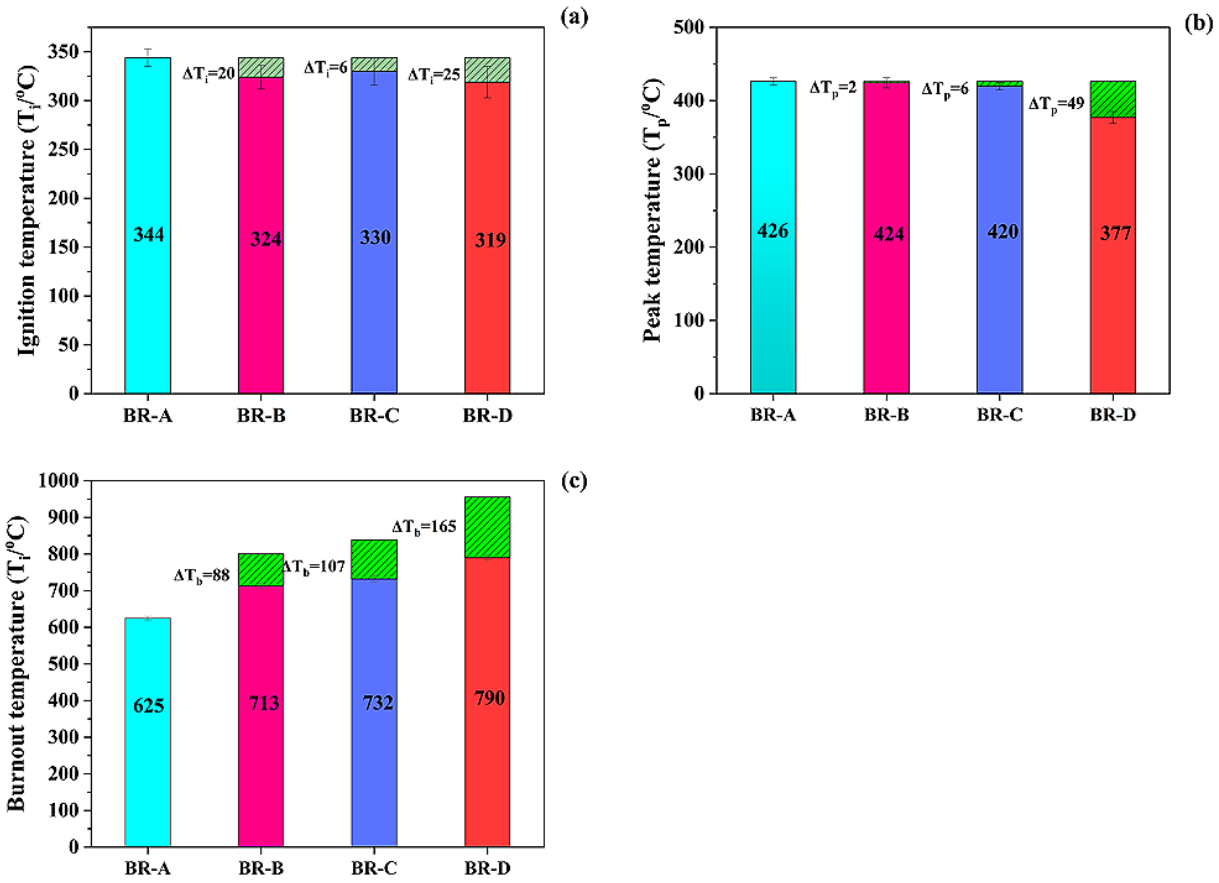

Figure 7 (a) Ignition temperature, (b) peak temperature, and (c) burnout temperature of the briquette types.

The presence of certain catalytic oxides like CaO, Fe_2O_3, and K_2O helps make the solid fuels easier to ignite, lowering the ignition temperature [43, 44]. Looking at the ash composition of the briquettes, shown in Table 2, BR-D's ash contains a good amount of CaO (26.55%), Fe_2O_3 (24.50%), and K_2O (12.70%), with only a small amount of TiO_2 (2.91%). These ingredients likely work together to help BR-D ignite at the lowest temperature observed. On the other hand, the ash from BR-A is mostly composed of titanium compounds, with TiO_2 making up 40.25%. Since titanium compounds are known to slow down biomass combustion [45]. This probably explains why BR-A takes longer to ignite, at around 344°C.

The ashes of BR-B and BR-C also contain significant amounts of CaO, Fe_2O_3, and K_2O. Their catalytic effects likely help these briquettes ignite more easily, which is why their ignition temperatures are lower than those of BR-A.

Figure 7b shows the peak temperatures (T_p) during combustion for briquettes from BR-A to BR-D. As can be observed, briquettes that contain plastics have lower peak temperatures than BR-A, which is made entirely from sawdust. According to Table 3, the greater the PET content in the briquettes, the higher the volatile matter (VM) content. Since VM is released early during burning, it generates heat that helps preheat the remaining carbon, making it easier to ignite. This process explains why plastic-rich briquettes have a lower peak temperature. BR-D, which has the most plastic, reaches the lowest peak temperature of 377°C. The difference in peak temperatures between BR-A and BR-D is quite significant (ranging from 2 to 49°C), showing a strong link between plastic content and peak temperature.

Figure 7c shows the burnout temperatures (T_b), which indicate how much heat is needed to completely burn out the briquettes. These temperatures increase as PET content rises, especially for BR-D. The higher residual heat suggests that PET plastic contributes to more stable, longer-lasting combustion due to its thermal stability and ability to form char or other residues that require higher temperatures to fully burn out [46]. The amount of char residue also increases with PET content: about 4.45% for BR-A, 6.01% for BR-B, 8.32% for BR-C, and 24.83% for BR-D. Generally, more char residue is associated with a higher heating value (HHV) [46, 47], which aligns with the trend seen in the residual weights and energy content across these briquettes. Similar relationships between char and HHV have been reported in other studies, like Liu et al. [21], who examined briquettes made from corn straw.

Overall, adding PET plastic alters the thermal behaviour of the briquettes by making them easier to ignite and promoting more complete burning at higher residual heat levels. This suggests that PET acts as a kind of combustion enhancer, enabling quicker ignition and more efficient, cleaner burning. These effects are important for designing briquettes tailored for specific uses, especially where fast ignition and steady, long-lasting combustion with minimal emissions are desired.

3.7.2 Effect of Plastic Concentration on Combustion Performance Indices

Table 7 highlights the combustion performance indices of the produced briquette types (BR-A to BR-D), computed from TG-DTG curves. The results include important combustion parameters, such as the ignition index (D_i), burnout index (D_b), and burning rate intensity (H_f), which are defined by Equations (3)-(5). These parameters help understand the ease of ignition, combustion stability, and overall combustion performance of each briquette.

Table 7 Key combustion performance indices for the briquettes.

Briquette	Ignition index (D_i) (% min^{-2} $°C^{-1}$)	Burnout index (D_b) (% $°C^{-1}$ min^{-3})	burning rate intensity (H_f) (°C)
BR-A	0.0283	2.631E-03	1.564
BR-B	0.0318	2.1931E-03	1.557
BR-C	0.0321	2.1870E-03	1.502
BR-D	0.0466	4.005E-03	1.132

The ignition index indicates a material's ability to release volatiles, which directly affects ignition and combustion stability [48, 49]. An increase in D_i means an increase in volatile release capacity and, therefore, an increase in ignition capacity [50]. The effect of VM content on ignition performance is evident in the D_i values; the BR-D, with a VM content of 85.19%, has the largest D_i value of about 0.0466. This implies that BR-D will ignite more easily than others. Better ignition characteristics are beneficial in quick start-up in cooking applications, reducing waiting time. As shown in Table 7, the greater the plastic content, the larger D_i.

The burnout process is defined by D_b, which is a factor that relies on T_b and T_p. Reduced T_b values permit faster burnout, since unburned compounds are burned more rapidly. Conversely, higher burnout temperatures imply longer process times that require high temperatures and prolonged residence times [51, 52]. Table 6 indicates that the burnout temperature of BR-A to BR-D increases with the percentage of plastics in the mixture; therefore, the burnout index of BR-A to BR-D rises

with the percentage of plastics in the mixture, with BR-D having the highest T_b (790°C) and D_b (4.005E-03), indicating high combustion reactivity. The H_f index is used to determine the rate and intensity of combustion, and the lower the H_f, the more efficient the combustion [53]. The H_f index of BR-A is approximately 1.564, and that of BR-D is approximately 1.132, which means that BR-D may generate a more constant heat production as opposed to burning intensely. The same trends have been noted in comparative studies of coal and biomass combustion [20, 52, 54]. Based on these results, it can be concluded that incorporating plastics into the briquette mixture enhances their combustion characteristics and performance, indicating good prospects for energy applications.

3.8 Kinetic Analysis

The combustion kinetics of the four briquettes (BR-A to BR-D) were determined using data from the thermogravimetric analysis. An Arrhenius-type kinetic model was employed to analyse the TG-DTG data. As shown in Figure 6, the DTG curves for the four briquettes, measured at a constant heating rate of 10°C/min, exhibit single, bell-shaped peaks without shoulders across the temperature range from ignition to burnout. This suggests that the combustion process for all four briquettes proceeded as a single-step reaction, consistent with established methods for identifying single-step kinetics [54, 55]. The Coats-Redfern method was applied to analyse the combustion region, assuming the process follows a first-order kinetic reaction. While we acknowledge the concerns raised by the ICTAC Kinetics Committee regarding the limitations of single-heating-rate methods, such as their potential difficulty in accurately determining kinetic triplets due to the complex nature of biomass combustion, the Coats-Redfern method was chosen based on practical considerations. The Coats-Redfern technique is useful for initial assessments when approximate kinetic parameters surffice, enabling meaningful comparisons among different biomass types under similar conditions. Moreover, conducting experiments at various heating rates requires significant time, resources, and specialised equipment, which is quite taxing. Additionally, analysing data at a single heating rate mirrors a real-world briquette combustion scenario, where processes typically occur under constant heating conditions, thus increasing the relevance of the findings from this study. Despite its limitations, the Coats-Redfern method has been demonstrated to be reliable in numerous studies when applied with an awareness of its constraints [22, 25, 56-58]. Figure 8 presents the results of fitting the conversion rate data (x) as a function of reaction temperature (T) for briquettes BR-A to BR-D. The correlation coefficients ranged from 0.9598 to 0.9803.

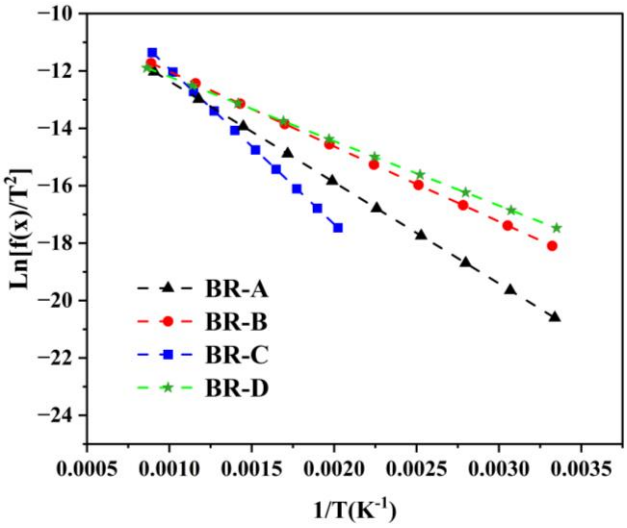

Figure 8 Kinetic plots for the produced briquettes.

Using the Coats-Redfern method at a heating rate of 10°C/min, the activation energies (E_a) for the four briquettes were calculated and are summarised in Table 8.

Table 8 Activation energies of the produced briquettes.

	Briquette			
E_a (kJ/mol)	BR-A	BR-B	BR-C	BR-D
	29.31	21.74	20.09	18.67

The results indicate that the E_a values for briquettes with plastic (BR-B to BR-D) range from 18.67 to 21.74 kJ/mol, and are lower than that of BR-A, without plastic (29.31 kJ/mol). The observed trend suggests that increasing the PET plastic content reduces the activation energy required for the briquettes' combustion process. The key reason for the decrease in activation energy is the strong synergistic physical and chemical interactions between the decomposing biomass and plastic materials, which promote increased carbon conversion efficiency and a higher yield of volatile products compared to the combustion of biomass or plastic alone [59-62]. For instance, kinetic studies by Mishra et al. [61] demonstrated that blending Samanea saman seeds (SS) with PET plastic at a 3:1 ratio required a lower activation energy to initiate degradation than either component alone. Oyedun et al. [62] reported that increasing the plastic content in mixtures of sawdust and HDPE reduced the activation energy required to initiate the decomposition reaction. Similarly, Burra and Gupta [59] observed that blending polycarbonate with pinewood reduced the activation energy of the polycarbonate by about 50 kJ/mol, compared to the degradation of the individual polymer. The addition of PET plastic improved the reactivity of the briquettes during thermal decomposition, a trend that aligns well with observations from our study.

3.9 Water Boiling Test Performance Metrics

Table 9 presents the performance of briquettes BR-A to BR-D during the various WBT phases: cold start, hot start, and simmer, focusing on important parameters such as time to boil, burning rate, fuel consumption, energy efficiency, and firepower.

Table 9 WBT performance metrics variables for the developed briquettes.

WBT Phase	Performance metrics variables	BR-A	BR-B	BR-C	BR-D
Cold start	Time to boil (min)	38	36	32	30
	Burning rate (g/min)	1.87	1.85	1.74	1.66
	Specific fuel consumption (g/L)	59.60	52.50	45.70	40.20
	Specific energy consumption (kJ/L)	1.314	1.247	1.115	1.048
	Thermal efficiency (%)	46.05	49.12	52.21	54.05
	Firepower (W)	623.33	638.52	641.48	654.32
Hot start	Time to boil (min)	33	31	27	25
	Burning rate (g/min)	1.91	1.89	1.78	1.70
	Specific fuel consumption (g/L)	56.50	49.40	42.60	37.10
	Specific energy consumption (kJ/L)	1.246	1.121	1.039	0.967
	Thermal efficiency (%)	49.21	52.15	55.23	57.05
	Firepower (W)	636.67	643.49	656.23	670.08
Simmer	Burning rate (g/min)	0.39	0.36	0.31	0.28
	Specific fuel consumption (g/L)	6.50	6.15	5.50	5.25
	Specific energy consumption (kJ/L)	0.143	0.136	0.134	0.132
	Thermal efficiency (%)	62.15	65.27	70.02	73.14
	Firepower (kW)	130.00	129.30	114.29	110.37

For the cold start high power phase, the time to boil reduced from BR-A to BR-D, implying enhanced heating performance. The burning rate and fuel consumption were lower, suggesting better combustion, and the thermal efficiency increased with the proportion of PET plastic, reaching above 54% in BR-D. Similar trends were observed in hot start, with reduced boiling time and improved efficiency. BR-D consistently exhibited the best performance, consuming less fuel and energy per liter, and having greater thermal efficiency. The burning rate and fuel consumption were much lower during simmering, indicating energy conservation. The thermal efficiency continues to increase to more than 73% in BR-D. The firepower was slightly reduced, which was appropriate to keep the heat at a constant low level.

In general, BR-D consistently outperforms the other briquettes across all the stages: it uses less fuel, has higher thermal efficiencies, and boils more quickly. This indicates that BR-D is more efficient in energy consumption, cheaper, and can heat quickly and simmer for a long time, hence it is more ideal for clean cooking [39, 63].

3.10 Energetic Properties of Developed Briquettes

Table 10 presents the energetic properties of the developed briquettes BR-A to BR-D. The data show a clear trend of increasing energetic density and Fuel Value Index (FVI) from BR-A to BR-D.

Table 10 Energetic properties of the developed briquettes.

Energetic Properties	BR-A	BR-B	BR-C	BR-D
Energetic density (GJ/m^3)	12.96	14.45	15.69	16.93
Fuel Value Index (GJ/m^3%)	2.37	4.62	5.32	6.46

These parameters are essential indicators of the energy storage capacity, combustion efficiency, and general applicability of the briquettes across various applications. Energetic density increases to 16,929.38 MJ/m^3 in BR-D as compared to 12,962.40 MJ/m^3 in BR-A. An increase in the energetic density means that more energy is stored in a given volume. This increase enhances the efficiency of storage and transport since less volume is needed to produce the same energy output [39]. It also indicates better packing and densification of the briquettes, which may be because of the presence of PET particles or to superior production methods. The FVI rises from 2,365.40 MJ/m^3% in BR-A to 6,461.59 MJ/m^3% in BR-D. The Fuel Value Index (FVI) essentially measures how much energy a briquette contains based on its volume. The higher the FVI, the more efficient the briquette is at burning and the greater its potential to produce heat. Briquettes with a higher FVI are especially suitable for applications that require a lot of heat or long-lasting heat output [63]. The changes in energy properties observed are likely connected to physical changes in the briquettes' structure (as shown in Figure 5). These include becoming denser, having fewer pores, and forming stronger bonds between particles. All of these factors help improve how well the briquettes burn and how much energy they retain during combustion.

4. Conclusions

Thermogravimetric analysis was done to explore how different amounts of PET plastics affect the combustion behavior and kinetics of waste-derived briquettes made from blends of sawdust and waste PET plastics. To assess the efficiency and energy consumption of these briquettes, a water boiling test (WBT) was conducted. Four types of briquettes were produced by high-pressure compaction with different mass ratios of the raw materials without binders. The SEM micrographs showed that adding PET improved the internal bonding between particles and reduced porosity, making the briquettes stronger, more durable, and more stable during burning. Overall, the presence of PET significantly influenced their thermal properties by lowering the ignition temperature, decreasing the energy required to initiate combustion, and increasing the temperature at which they are completely burned out. For example, BR-D had the lowest ignition index (0.0466% min^{-2} $°C^{-1}$), the lowest activation energy (18.67 kJ/mol), and the highest burnout index (4.005E-03% $°C^{-1}$ min^{-3}), which implies fast ignition and robust combustion, although it surprisingly had the highest char residue. In all stages of the WBT, BR-D was always superior to the other briquettes in terms of less fuel, higher thermal efficiencies, and faster boiling of water. These characteristics make BR-D especially appropriate for quick heating and prolonged simmering, which are ideal for clean cooking. Furthermore, BR-D showed the best energy potential with the highest energetic density (16.93 GJ/m^3) and fuel value index (6.46 GJ/m^3%).

These results are relevant to the development of waste-to-energy conversion technologies and demonstrate that a mixture of sawdust and PET can be used to optimize combustion and increase energy yield during briquette burning. Future research will involve a life-cycle assessment (LCA) to assess the environmental impact of the briquette production.

Acknowledgments

The authors would like to appreciate the financial contributions of the World Bank Centre of Excellence in Reproductive Health Initiative (CERHI), University of Benin, towards the success of this project.

Author Contributions

Peter Ebhodaghe Akhator: Conceptualisation, Methodology, Data curation, Formal analysis, Supervision, Writing (original draft, review and editing), Resources. Ufuoma Georgina Unueroh: Conceptualisation, Methodology, Data curation, Formal analysis, Writing (original draft, review and editing), Resources.

Competing Interests

The authors declare that the study was carried out without any commercial or financial relationships that could present a potential conflict of interest.

Data Availability Statement

Data will be made available on request.

AI-Assisted Technologies Statement

During the preparation of this work, the authors used an artificial intelligence tool (OpenAI) to improve the language and readability. After using this tool, the authors reviewed and edited the content as needed and take full responsibility for the content of the publication.

References

1. Nath B, Chen G, Bowtell L, Mahmood RA. Assessment of densified fuel quality parameters: A case study for wheat straw pellet. J Bioresour Bioprod. 2023; 8: 45-58.
2. Yiga VA, Nuwamanya A, Birungi A, Lubwama M, Lubwama HN. Development of carbonized rice husks briquettes: Synergy between emissions, combustion, kinetics and thermodynamic characteristics. Energy Rep. 2023; 9: 5977-5991.
3. Alam MT, Lee JS, Lee SY, Bhatta D, Yoshikawa K, Seo YC. Low chlorine fuel pellets production from the mixture of hydrothermally treated hospital solid waste, pyrolytic plastic waste residue and biomass. Energies. 2019; 12: 4390.
4. Cesprini E, Greco R, Causin V, Urso T, Cavalli R, Zanetti M. Quality assessment of pellets and briquettes made from glued wood waste. Eur J Wood Wood Prod. 2021; 79: 1153-1162.
5. Faisal RM, Ardian A, Khoiriyah V, Chafidz A. Production of briquettes from a blend of HDPE (high density polyethylene) plastic wastes and teak (*Tectona grandis* Linn. f) sawdust using different natural adhesives as the binder. Key Eng Mater. 2021; 882: 273-279.
6. Munsin R, Udtasri J, Topaiboul S, Kowtakul P, Yeunyongkul P, Nuntapap N, et al. A study on binderless co-pelletization of industrial rice-powder wastes and teak sawdust at low and elevated temperatures. Case Stud Chem Environ Eng. 2022; 6: 100250.
7. Qi J, Li H, Wang Q, Han K. Combustion characteristics, kinetics, SO_2 and NO release of low-grade biomass materials and briquettes. Energies. 2021; 14: 2655.
8. Emadi B, Iroba KL, Tabil LG. Effect of polymer plastic binder on mechanical, storage and combustion characteristics of torrefied and pelletized herbaceous biomass. Appl Energy. 2017; 198: 312-319.

9. Widyanto H, Wijianto. Enhance residual quality: Experimental study of briquettes based on husks and plastic. AIP Conf Proc. 2022; 2566: 090003.
10. Sawadogo M, Tanoh ST, Sidibé S, Kpai N, Tankoano I. Cleaner production in Burkina Faso: Case study of fuel briquettes made from cashew industry waste. J Clean Prod. 2018; 195: 1047-1056.
11. Kosajan V, Wen Z, Fei F, Dinga CD, Wang Z, Zhan J. The feasibility analysis of cement kiln as an MSW treatment infrastructure: From a life cycle environmental impact perspective. J Clean Prod. 2020; 267: 122113.
12. Mong OO, Obi OE, Onyeocha CE, Ndubuisi CO, Gaven DV, Nnadiegbulam V. An experimental studyon biomass fuel briquettes' quality as a product of waste conversion in Nekede, Owerri, Nigeria. J Energy Res Rev. 2023; 14: 22-31.
13. Sotannde OA, Oluyege AO, Abah GB. Physical and combustion properties of briquettes from sawdust of *Azadirachta indica*. J For Res. 2010; 21: 63-67.
14. Cheremisinoff NP. Chapter 1—Source reduction and waste minimization. In: Handbook of solid waste management and waste minimization technologies. Burlington: Butterworth-Heinemann; 2003. pp. 1-22.
15. Sintim HY, Bary AI, Hayes DG, English ME, Schaeffer SM, Miles CA, et al. Release of micro-and nanoparticles from biodegradable plastic during in situ composting. Sci Total Environ. 2019; 675: 686-693.
16. Akhator PE, Bazuaye L, Ewere A, Oshiokhai O. Production and characterisation of solid waste-derived fuel briquettes from mixed wood wastes and waste pet bottles. Heliyon. 2023; 9: e21432.
17. Zahra NL, Septiariva IY, Sarwono A, Qonitan FD, Sari MM, Gaina PC, et al. Substitution garden and polyethylene terephthalate (PET) plastic waste as refused derived fuel (RDF). Int J Renew Energy Dev. 2022; 11: 523-532.
18. Nakiyinji J. Development and characterization of composite briquettes for domestic cooking application. Kampala, Uganda: Makerere University; 2022.
19. Yiga VA, Lubwama M. Thermogravimetric analysis of agricultural residue carbonized briquettes for domestic and industrial applications. MRS Adv. 2020; 5: 1039-1048.
20. Jia G. Combustion characteristics and kinetic analysis of biomass pellet fuel using thermogravimetric analysis. Processes. 2021; 9: 868.
21. Liu J, Jiang X, Cai H, Gao F. Study of combustion characteristics and kinetics of agriculture briquette using thermogravimetric analysis. ACS Omega. 2021; 6: 15827-15833.
22. Bongomin O, Nzila C, Mwasiagi JI, Maube O. Comprehensive thermal properties, kinetic, and thermodynamic analyses of biomass wastes pyrolysis via TGA and Coats-Redfern methodologies. Energy Convers Manag X. 2024; 24: 100723.
23. Yuanyuan Z, Yanxia G, Fangqin C, Kezhou Y, Yan C. Investigation of combustion characteristics and kinetics of coal gangue with different feedstock properties by thermogravimetric analysis. Thermochim Acta. 2015; 614: 137-148.
24. Lei J, Liu X, Xu B, Liu Z, Fu Y. Combustion characteristics, kinetics and thermodynamics of peanut shell for its bioenergy valorization. Processes. 2024; 12: 1022.
25. Li BY, Tee MY, Nge KS, Ng AK, Chong WW, Ng JH, et al. Comparison kinetic analysis between Coats-Redfern and Criado's master plot on pyrolysis of horse manure. Chem Eng Trans. 2023; 106: 1273-1278.

26. Gajera ZR, Verma K, Tekade SP, Sawarkar AN. Kinetics of co-gasification of rice husk biomass and high sulphur petroleum coke with oxygen as gasifying medium via TGA. Bioresour Technol Rep. 2020; 11: 100479.
27. Liang W, Wang G, Jiao K, Ning X, Zhang J, Guo X, et al. Conversion mechanism and gasification kinetics of biomass char during hydrothermal carbonization. Renew Energy. 2021; 173: 318-328.
28. Arora P, Das P, Jain S, Kishore VV. A laboratory based comparative study of Indian biomass cookstove testing protocol and Water Boiling Test. Energy Sustain Dev. 2014; 21: 81-88.
29. Luo J, Li Q, Meng A, Long Y, Zhang Y. Combustion characteristics of typical model components in solid waste on a macro-TGA. J Therm Anal Calorim. 2018; 132: 553-562.
30. Zhao L, Giannis A, Lam WY, Lin SX, Yin K, Yuan GA, et al. Characterization of Singapore RDF resources and analysis of their heating value. Sustain Environ Res. 2016; 26: 51-54.
31. Dalimunthe YK, Satiawati L, Widiyatni H, Dahani W, Rahman MA, Nursyam SS, et al. Effect of adding LDPE, PP and biodegradable plastic waste on physical properties, calorific value and proximate analysis of peanut shell waste briquettes. Int J Eng Trans A Basics. 2025; 38: 54-64.
32. Edo M, Budarin V, Aracil I, Persson PE, Jansson S. The combined effect of plastics and food waste accelerates the thermal decomposition of refuse-derived fuels and fuel blends. Fuel. 2016; 180: 424-432.
33. Reza MT, Rottler E, Herklotz L, Wirth B. Hydrothermal carbonization (HTC) of wheat straw: Influence of feedwater pH prepared by acetic acid and potassium hydroxide. Bioresour Technol. 2015; 182: 336-344.
34. Reza MT, Wirth B, Lüder U, Werner M. Behavior of selected hydrolyzed and dehydrated products during hydrothermal carbonization of biomass. Bioresour Technol. 2014; 169: 352-361.
35. Guo F, Miao Z, Guo Z, Li J, Zhang Y, Wu J. Properties of flotation residual carbon from gasification fine slag. Fuel. 2020; 267: 117043.
36. Akhator P, Oboirien B, Borhani TN. Interaction effects between sugarcane bagasse and sawdust during their co-hydrothermal carbonisation and co-gasification. Energy Convers Manag X. 2025; 28: 101247.
37. Stelte W, Clemons C, Holm JK, Ahrenfeldt J, Henriksen UB, Sanadi AR. Fuel pellets from wheat straw: The effect of lignin glass transition and surface waxes on pelletizing properties. Bioenergy Res. 2012; 5: 450-458.
38. Geberehiet GA, Gebreegziabher TG, Mekonen AG, Hagos GK, Gebresilasie TN. Development of briquettes suitable for energy generation from residue of sorghum stalk and groundnut husk. Mater Renew Sustain Energy. 2025; 14: 35.
39. Dorokhov VV, Nyashina GS, Romanov DS, Strizhak PA. Combustion and mechanical properties of pellets from biomass and industrial waste. Renew Energy. 2024; 228: 120625.
40. EN*plus* Handbook. Part 3–Pellet quality requirements [Internet]. Brussels, Belgium: European Pellet Council; 2015. Available from: https://nencom.com/f/products/pellets/enplus/enplus-3-v3-inter-en.pdf.
41. Carnaje NP, Talagon RB, Peralta JP, Shah K, Paz-Ferreiro J. Development and characterisation of charcoal briquettes from water hyacinth (*Eichhornia crassipes*)-molasses blend. PLoS One. 2018; 13: e0207135.

42. Hu M, Deng W, Hu M, Chen G, Zhou P, Zhou Y, et al. Preparation of binder-less activated char briquettes from pyrolysis of sewage sludge for liquid-phase adsorption of methylene blue. J Environ Manag. 2021; 299: 113601.
43. Feng S, Yuan Z, Leitch M, Xu CC. Hydrothermal liquefaction of barks into bio-crude–Effects of species and ash content/composition. Fuel. 2014; 116: 214-220.
44. Zhang S. Effects of ash/K_2CO_3/Fe_2O_3 on ignition temperature and combustion rate of demineralized anthracite. J Fuel Chem Technol. 2014; 42: 166-174.
45. Kumar J, Vyas S. Comprehensive review of biomass utilization and gasification for sustainable energy production. Environ Dev Sustain. 2025; 27: 1-40.
46. Rantuch P. The thermal degradation of polymer materials. In: Ignition of polymers. Cham: Springer International Publishing; 2022. pp. 1-43.
47. De Souza EC, Gomes JP, Pimenta AS, De Azevedo TK, Pereira AK, Gomes RM, et al. Briquette production as a sustainable alternative for waste management in the tannin extraction industry. Environ Sci Pollut Res. 2023; 30: 18078-18090.
48. Liu Y, Cao X, Duan X, Wang Y, Che D. Thermal analysis on combustion characteristics of predried dyeing sludge. Appl Therm Eng. 2018; 140: 158-165.
49. Sieradzka M, Mlonka-Mędrala A, Kalemba-Rec I, Reinmöller M, Küster F, Kalawa W, et al. Evaluation of physical and chemical properties of residue from gasification of biomass wastes. Energies. 2022; 15: 3539.
50. Li XG, Lv Y, Ma BG, Jian SW, Tan HB. Thermogravimetric investigation on co-combustion characteristics of tobacco residue and high-ash anthracite coal. Bioresour Technol. 2011; 102: 9783-9787.
51. Nguyen HL, Le DD, Nguyen HN, Trinh VT. Thermal behavior of woody biomass in a low oxygen atmosphere using macro-thermogravimetric analysis. GMSARN Int J. 2020; 14: 37-41.
52. Mureddu M, Dessì F, Orsini A, Ferrara F, Pettinau A. Air-and oxygen-blown characterization of coal and biomass by thermogravimetric analysis. Fuel. 2018; 212: 626-637.
53. Niu S, Lu C, Han K, Zhao J. Thermogravimetric analysis of combustion characteristics and kinetic parameters of pulverized coals in oxy-fuel atmosphere. J Therm Anal Calorim. 2009; 98: 267-274.
54. Tang L, Xiao J, Mao Q, Zhang Z, Yao Z, Zhu X, et al. Thermogravimetric analysis of the combustion characteristics and combustion kinetics of coals subjected to different chemical demineralization processes. ACS Omega. 2022; 7: 13998-14008.
55. Vyazovkin S, Burnham AK, Favergeon L, Koga N, Moukhina E, Pérez-Maqueda LA, et al. ICTAC Kinetics Committee recommendations for analysis of multi-step kinetics. Thermochim Acta. 2020; 689: 178597.
56. Monir MU, Shovon SM, Akash FA, Habib MA, Techato K, Abd Aziz A, et al. Comprehensive characterization and kinetic analysis of coconut shell thermal degradation: Energy potential evaluated via the Coats-Redfern method. Case Stud Therm Eng. 2024; 55: 104186.
57. Ferfari O, Belaadi A, Bourchak M, Ghernaout D, Ajaj RM, Chai BX. Thermal decomposition of *Syagrus romanzoffiana* palm fibers: Thermodynamic and kinetic studies using the coats-redfern method. Renew Energy. 2024; 231: 120928.
58. Wu S, Wang Q, Cui D, Sun H, Yin H, Xu F, et al. Evaluation of fuel properties and combustion behaviour of hydrochar derived from hydrothermal carbonisation of agricultural wastes. J Energy Inst. 2023; 108: 101209.

59. Burra KG, Gupta AK. Kinetics of synergistic effects in co-pyrolysis of biomass with plastic wastes. Appl Energy. 2018; 220: 408-418.
60. Kumar A, Swarnalatha AP, Shwetha J, Saravanan P, Hatamleh AA, Al-Dosary MA, et al. Pyrolysis behaviour and synergistic effect in co-pyrolysis of wheat straw and polyethylene terephthalate: A study on product distribution and oil characterization. Heliyon. 2024; 10: e37255.
61. Mishra RK, Sahoo A, Mohanty K. Pyrolysis kinetics and synergistic effect in co-pyrolysis of *Samanea saman* seeds and polyethylene terephthalate using thermogravimetric analyser. Bioresour Technol. 2019; 289: 121608.
62. Oyedun AO, Tee CZ, Hanson S, Hui CW. Thermogravimetric analysis of the pyrolysis characteristics and kinetics of plastics and biomass blends. Fuel Process Technol. 2014; 128: 471-481.
63. Vaish S, Sharma NK, Kaur G. A review on various types of densification/briquetting technologies of biomass residues. IOP Conf Ser Mater Sci Eng. 2022; 1228: 012019.